

UC San Diego

UC San Diego Previously Published Works

Title

Rapid Integration of Multi-copy Transgenes Using Optogenetic Mutagenesis in *Caenorhabditis elegans*.

Permalink

<https://escholarship.org/uc/item/95j39870>

Journal

G3 (Bethesda, Md.), 8(6)

ISSN

2160-1836

Authors

Noma, Kentaro
Jin, Yishi

Publication Date

2018-05-01

DOI

10.1534/g3.118.200158

Peer reviewed

Rapid Integration of Multi-copy Transgenes Using Optogenetic Mutagenesis in *Caenorhabditis elegans*

Kentaro Noma^{*,†,1,2,3} and Yishi Jin^{*,†,3}

^{*}Division of Biological Sciences, Neurobiology Section, University of California, San Diego, La Jolla, California 92093 and

[†]Howard Hughes Medical Institute, University of California, San Diego, La Jolla, CA 92093

ORCID IDs: 0000-0002-6487-8037 (K.N.); 0000-0002-9371-9860 (Y.J.)

ABSTRACT Stably transmitted transgenes are indispensable for labeling cellular components and manipulating cellular functions. In *Caenorhabditis elegans*, transgenes are generally generated as inheritable multi-copy extrachromosomal arrays, which can be stabilized in the genome through a mutagenesis-mediated integration process. Standard methods to integrate extrachromosomal arrays primarily use protocols involving ultraviolet light plus trimethylpsoralen or gamma- or X-ray irradiation, which are laborious and time-consuming. Here, we describe a one-step integration method, following germline-mutagenesis induced by mini Singlet Oxygen Generator (miniSOG). Upon blue light treatment, miniSOG tagged to histone (Histone-miniSOG) generates reactive oxygen species (ROS) and induces heritable mutations, including DNA double-stranded breaks. We demonstrate that we can bypass the need to first establish extrachromosomal transgenic lines by coupling microinjection of desired plasmids with blue light illumination on Histone-miniSOG worms to obtain integrants in the F₃ progeny. We consistently obtained more than one integrant from 12 injected animals in two weeks. This optogenetic approach significantly reduces the amount of time and labor for transgene integration. Moreover, it enables to generate stably expressed transgenes that cause toxicity in animal growth.

KEYWORDS

C. elegans
transgene
integration
optogenetic
mutagenesis
miniSOG

Transgenesis provides a powerful means to transfer desired genetic materials into an organism. Transgenes expressing fluorescent reporters are essential for visualization of tissues, cells, subcellular structures or protein localizations; and transgenes overexpressing a gene of interest are necessary to investigate genetic pathways in many biological processes. In *Caenorhabditis elegans*, transgenesis can be quickly accomplished

following microinjection of DNAs into the germline, which then form heritable extrachromosomal arrays (Mello *et al.* 1991; Evans 2006). Such extrachromosomal transgenes, however, frequently display mosaic expression due to stochastic loss during cell division in somatic and germline cells, as well as variability in expression levels. While Clustered Regularly Interspersed Short Palindromic Repeats (CRISPR)-based knock-in (Kim *et al.* 2014; Paix *et al.* 2014; Paix *et al.* 2015) and Mos1-mediated Single-Copy Insertion (MosSCI) (Frøkjær-Jensen *et al.* 2008; Frøkjær-Jensen *et al.* 2014) have tremendous value for stable expression from endogenous or defined loci, expression levels of such transgenes might be too low for visual detection or may not induce desired overexpression. Thus, integration of high-copy extrachromosomal transgenes remains necessary to achieve stable and high expression. Traditionally, ultraviolet with trimethylpsoralen (UV/TMP) or gamma- or X-ray irradiation has been used to integrate transgenes (Evans 2006). These methods are laborious and time-consuming, requiring the establishment of extrachromosomal transgenic lines before integration (Figure 1A).

The Light-oxygen-voltage-sensing (LOV) domain-derived Mini Singlet Oxygen Generator (miniSOG) generates reactive oxygen species (ROS) upon blue-light illumination (Shu *et al.* 2011).

Copyright © 2018 Noma and Jin

doi: <https://doi.org/10.1534/g3.118.200158>

Manuscript received February 15, 2018; accepted for publication April 18, 2018; published Early Online April 24, 2018.

This is an open-access article distributed under the terms of the Creative Commons Attribution 4.0 International License (<http://creativecommons.org/licenses/by/4.0/>), which permits unrestricted use, distribution, and reproduction in any medium, provided the original work is properly cited.

Supplemental material available at Figshare: <https://doi.org/10.25387/g3.6127709>.

¹Current address: Group of Nutritional Neuroscience, Division of Biological Science, Graduate School of Science, Nagoya University, Nagoya, Aichi, Japan 464-8602

²Japan Science and Technology Agency, Kawaguchi, Saitama, Japan 332-0012

³Co-correspondence to: Yishi Jin, University of California, San Diego, Neurobiology Section, 9500 Gilman Drive, La Jolla, CA 92093-0368, E-mail: yijin@ucsd.edu, Kentaro Noma, Nagoya University, School of Science Building B, Room 103, Furo-cho, Chikusa-ku, Nagoya, Japan 464-8602, E-mail: noma.kentaro@e.mbox.nagoya-u.ac.jp

A

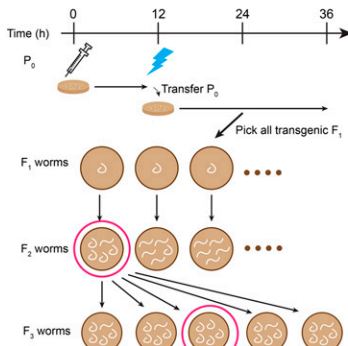
Traditional UV/TMP integration

Day1: Inject DNA
Day4: Pick transgenic F_1
Day7: Find F_1 plates with heritable transgene
Amplify # of worms
Day10: Treat with UV/TMP
Day13: Pick transgenic F_1
Day16: Find F_1 plates with high transmission rate
Day19: Find F_2 plates with 100% transmission rate

Optogenetic integration

Day1: Inject DNA
Day1: Treat with light
Day4: Pick transgenic F_1
Day7: Find F_1 plates with high transmission rate
Day10: Find F_2 plates with 100% transmission rate

B



C

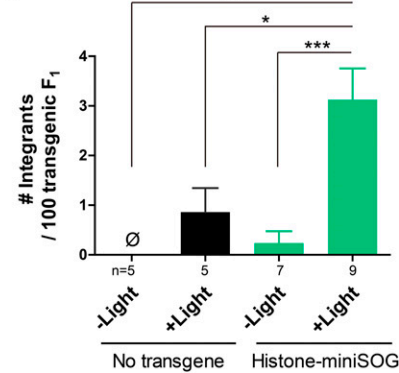


Figure 1 Schematic and efficiency of optogenetic integration. (A) Comparison of the workflow between a traditional UV/TMP method and optogenetic integration. (B) Schematic of optogenetic integration with roller worms as an example of transgenic worms. Illuminating worms with blue light 12 hr after microinjection, parental worms were transferred to new plates. A few days later, transgenic F_1 worms were singly plated. From F_1 plates with high transmission rate, five transgenic F_2 worms were singly plated and examined for 100% transmission rate. The progeny before light treatment was also examined to determine the light dependency of the method. (C) Efficiency of integration was calculated as the number of integrants per 100 transgenic F_1 progeny. n indicates the number of experiments (12 worms for microinjection/experiment). Error bars indicate S.E.M. Statistics: one-way ANOVA followed by Dunnett's test, * $P < 0.05$, *** $P < 0.001$.

Previously, we have established a method called “optogenetic mutagenesis”, in which miniSOG fused to a histone is expressed in the germline of *C. elegans*, and induces heritable mutations following blue-light illumination with the estimated loss-of-function mutation frequency to be 0.72 ± 0.14 per 1,000 haploid genomes (Noma and Jin 2015; Noma and Jin 2016). We showed that this optogenetic mutagenesis could also induce integration of extrachromosomal transgenes at a frequency comparable to that using the traditional UV/TMP protocol (Noma and Jin 2015). Here, we significantly improved this approach and demonstrated that establishment of extrachromosomal transgenic lines can be bypassed by coupling microinjection of DNA plasmids with optogenetic mutagenesis in the parental generation. On average, we obtained more than one integrant from the progeny of twelve injected parental worms in two weeks. Moreover, by circumventing the establishment of extrachromosomal transgenic lines, we show that this method has the benefit to integrate transgenes expressing proteins toxic to the development and growth of the organism.

MATERIALS AND METHODS

Strain maintenance

Caenorhabditis elegans strains were maintained at 22.5° on Nematode Growth Medium (NGM) plates with OP50 bacteria as previously reported (Brenner 1974). Worms were maintained in the dark except picking for maintenance and imaging. Although the Histone-miniSOG strain does not cause detectable amount of mutations with ambient light (Noma and Jin 2015), it is advised to remove the Histone-miniSOG transgene as well as other background mutations by outcrossing the integrants.

Plasmids and strains

Bristol N2 was used as the wild type strain. For microinjection and integration, we used CZ20310 *juSi164*[*Pmex-5-his-72::miniSOG-3' UTR(tbb-2)* + *C. briggsae* (Cbr)-*unc-119*(+)] III *unc-119(ed3)* III (Noma

and Jin 2015), which expresses the single-copy Histone-miniSOG transgene under the control of germline-active promoter and 3'UTR. In case a desired genetic background should be introduced on the chromosome III, we also generated a strain, NUJ4 *knjS11*[*Pmex-5-his-72::miniSOG-3' UTR(tbb-2)*] IV, which carries the single-copy Histone-miniSOG transgene. *rol-6(su1006dm)* (pRF4) (Mello *et al.* 1991) and *Pttx-3-RFP-3' UTR(unc-54)* plasmids were used to examine the efficiency of optogenetic integration. For GFP::RPS-18 expression, *Prps-18-GFP::rps-18* plasmid (pCZGY3162) (Noma *et al.* 2017) was used. To enhance the GFP::RPS-18 signals (Noma *et al.* 2017), *juIs531*[*GFP::rps-18* + *rol-6(su1006dm)*] transgene was examined in the *rps-18(ok3353)/nT1[qIs51 (Pmyo-2::GFP + Ppes-10::GFP + PF22B7.9::GFP)]* background. *Prgef-1-GFP::efa-6N-3' UTR(unc-54)* (pLC665) was made by recombination between GFP::*efa-6N* entry vector and *Prgef-1-GTW* destination vector using Gateway system (Invitrogen). pLC665 contains exons corresponding to the first 150 amino acids of EFA-6, which was fused to GFP with a 22 amino acid linker. For overexpressing *dlk-1*, we used pCZ848 expressing *Prgef-1-GFP::DLK-1L* and *Cbr-unc-119*, which was generated for MosSCI insertion (Holland *et al.* 2016). We note that *Cbr-unc-119* overexpression does not cause uncoordinated behavior.

Microinjection and optogenetic integration

Plasmid DNAs for microinjection were purified with QIAprep Spin Miniprep Kit (Qiagen), mixed at 100 ng/μl in total unless otherwise noted, and centrifuged at 15,000 rpm for 10 min at room temperature to avoid clogging microinjection needles. The plasmid solution was injected into the gonad of CZ20310 as previously described (Mello *et al.* 1991). We used non-gravid young adults for microinjection, which could be obtained by culturing worms at 22.5° approximately 50 hr post egg laying. Older worms can be used but the brood size would be decreased. Six to eighteen hours after microinjection, we illuminated worms with blue light at 2 mW/mm² and 4 Hz for 30 min as previously described (Noma and Jin 2015; Noma

and Jin 2016). These P₀ worms were recovered on new seeded plates after light illumination. A few days later, all transgenic F₁ worms were put on individual plates (F₁ plates). Among these F₁ plates, we selected the plates with >50% F₂ worms carrying transgenes and recovered single transgenic F₂ onto five individual plates. A few days later, we examined for 100% transgene-positive F₃ worms. The potential integrated strains were crossed to N2 males and confirmed for Mendelian segregation. We did not find any integrants having two integration sites based on the segregation. We note that integrants may not show 100% penetrance of phenotypes as described in Results and Discussion. To distinguish between true integrants and extrachromosomal array lines with high-transmission rate, we used a few ways in addition to outcross. First, if the transgenes have fluorescence, we examined them under an epifluorescence upright microscope instead of a fluorescent stereo scope. Integrants sometimes show 100% fluorescence of the transgene despite variable expression of a co-injection marker. Second, we picked animals without phenotypes of the co-injection marker and checked if they produced transgenic progeny. True integrants will produce marker-positive progeny from marker-negative parents.

Quantitative PCR

Twenty adults were picked and put into the lysis solution (10 mM Tris (pH 8.8), 50 mM KCl, 0.1% Triton X-100, 2.5 mM MgCl₂, 100 µg/mL Proteinase K). These worms were then lysed by incubating at 65° for 60 min and subsequently at 95° for 15 min for inactivation of Proteinase K. Two microliters of the worm lysis were used as the templates for quantitative PCR (qPCR) using iQ SYBR Green Supermix (Bio-Rad) and a C1000 thermal cycler (Bio-Rad) with CFX96 Real-Time system (Bio-Rad). The parameters for the qPCR were 95° for 3 min and 40 cycles of 95° for 10 sec and 55° for 30 sec. The following primers were used for detecting integrated transgenes as well as *rps-25* for the internal control: *rps-25*:

YJ12209 (TCACACCATCCGTCGTCTCTG) and YJ12211 (GACCTGTCCGTGATGATGAACG), *ttx-3*: YJ12212 (GAG-CATACGCTTCGTCGGACT) and YJ12213 (GGAAAGTCATGTTGC-GCGAGAG), *rol-6*: YJ12214 (AGGAAGGACCAGATGGGCAC) and YJ12215 (GGTGAAGCATCCTGTTGGTGG), *efa-6*: YJ12216 (GCATC-GAGCATTCACCCACATC) and YJ12217 (CGATGGAAAC-GAAACTCCCGC). Copy number of integrated transgenes was calculated by normalizing to N2 and *rps-25*.

Microscopy

Bright field images and a movie were obtained from young adults using a Stemi508 stereo microscope (Zeiss) and a digital camera L-835 (Hozan). For fluorescence imaging, worms were immobilized with 25%(v/v) of 50 nm polystyrene beads (Polysciences, Inc.) in M9 solution. Representative images were collected from young adults using a LSM710 confocal microscope (Zeiss) equipped with a 10x (NA = 0.3), 63x (NA = 1.4), or 100x (NA = 1.46) objective lens. The zoom function of ZEN software (Zeiss) was used for imaging cell bodies of mechanosensory ALM neurons. Single-plane images or maximum-intensity-projections obtained from several z-sections (0.5 or 1 µm/section) using ZEN software (Zeiss) were shown. Fluorescence intensities were analyzed after subtracting background signals using FIJI software (Schindelin et al. 2012).

Statistical analysis

We used one-way ANOVA followed by Dunnett's test to compare multiple samples and linear regression to examine correlation in GraphPad Prism 7.0 (GraphPad Software, La Jolla, CA).

Data availability

The authors state that all data necessary for confirming the conclusions presented in the article are represented fully within the article. Supplemental material available at Figshare: <https://doi.org/10.25387/g3.6127709>.

RESULTS AND DISCUSSION

Transgene integration can be coupled with plasmid microinjection

To bypass the establishment of transgenic lines carrying extrachromosomal arrays, we tested if coupling microinjection into the germline with miniSOG-mediated optogenetic mutagenesis could lead to integration of transgenes. We performed microinjection of plasmid DNAs containing *rol-6(su1006dm)*, which produces dominant roller (Rol) phenotype (Mello et al. 1991), and those containing *Pttx-3-RFP*, which labels AIY neurons, into the gonad of non-gravid adult hermaphrodites expressing single-copy Histone-miniSOG transgene in the germline (*Pmex-5-his-72::miniSOG*, see Materials and Methods)(Noma and Jin 2015). Microinjected P₀ animals were recovered on seeded for 6, 12, or 18 hr. We then illuminated these P₀ animals with blue light to activate miniSOG. Nuclear ROS induction by Histone-miniSOG probably causes double-strand breaks, which enable integration of microinjected plasmids (Noma and Jin 2015). Rol F₁ progeny from light-treated P₀ was singly propagated (F₁ plates), and the ratio of Rol F₂ progeny was examined (Figures 1A and 1B). In theory, if an F₁ animal has a heterozygous integrated transgene (Rol/+), ~75% of its F₂ worms should show Rol phenotypes. To avoid overlooking, we propagated any transgene-bearing F₂ worms with >50% transmission rate (Table 1, High F₂). If singly propagated Rol F₂ worms (F₂ plates) produced 100% Rol F₃ progeny, we treated them as potential integrants and proceeded to outcrossing of the F₃ lines to wild type, followed with confirmation of the Mendelian segregation of Rol. In all integrants identified by Rol, we observed red fluorescence in AIY neurons. These results suggest that the *rol-6(su1006dm)* and *Pttx-3-RFP* transgenes were co-integrated in the genome. We were able to obtain such integrants among progeny of P₀ animals that received blue light treatment 6, 12, or 18 hr after microinjection (Table 1). The highest number of integrants was obtained from P₀ treated 6 hr after microinjection, while a slightly higher ratio of integrants per transgenic F₁ was obtained from P₀ treated 12 hr after microinjection. As a control for blue-light dependency, we examined the F₁ progeny produced from the same P₀ animals before light treatment (Figure 1B and Table 1, no light), and found only one integrant from a total of 227 transgenic F₁ animals, which was likely generated spontaneously. In contrast, we obtained ten integrants from a total of 410 transgenic F₁ animals in the light-treated condition (Table 1, light), suggesting that the integration is light-dependent (see below). We named this process as “optogenetic integration”.

Optogenetic integration is efficient

We further quantified the efficiency of optogenetic integration. From 12 P₀ worms treated with blue light 12 hr after microinjection, we obtained 61.3 ± 11.5 transgenic F₁ worms (mean ± SEM, n = 9 experiments), and 12.2 ± 2.5 F₂ animals carrying germline transmittable transgenes with >50% transmission rate. Among them, we obtained 1.6 ± 0.3 integrants. Statistical analysis showed that the optogenetic integration depends on both Histone-miniSOG transgene and light illumination (Figure 1C). The efficiency calculated as the number of integrants per 100 F₁ transgenic worms (Figure 1C)

■ Table 1 Optogenetic integration with light treatment at different time after injection

Time (h) ^a	# P ₀ ^b	No light, # transgenic animals				Light, # transgenic animals			
		F ₁	F ₂	High F ₂	Integrand	F ₁	F ₂	High F ₂	Integrand
6	12	0	0	0	0	114	45	31	1
6	12	2	0	0	0	143	40	13	5
12	12	33	7	4	0	34	14	10	2
12	12	60	32	20	1	74	34	22	1
18	12	78	41	29	0	25	8	7	0
18	12	54	25	14	0	20	5	5	1
Total:		227	105	67	1	410	146	88	10

^aTime (h) = time of light illumination after injection.

^b# P₀ = number of injected animals.

The total plasmid concentration is 100 ng/μm for all conditions.

was approximately five times higher than that using UV/TMP method or using previously reported miniSOG-based method (Noma and Jin 2015).

We next examined the effect of the total plasmid DNA concentration for microinjection on the efficiency. Extrachromosomal arrays are not efficiently transmittable to F₂ generation when the total concentration of plasmids is lower than 100 ng/μl (Mello *et al.* 1991). Here, we reasoned that by microinjecting lower concentration of plasmids, the integrants might be enriched among transgenic F₂. To test this, we microinjected the plasmids with the total concentration of 10 ng/μl or 25 ng/μl to CZ20310 worms and illuminated them with blue light 12 hr after microinjection. As expected, the efficiency to obtain heritable F₂ transgenic animals was reduced (Table 1 and Table S1). However, the efficiency to obtain integrants was also significantly reduced, compared to the microinjection with 100 ng/μl of total plasmids (Table 1 and Table S1). Therefore, we conclude that about 100 ng/μl of plasmids in total is favorable for optogenetic integration.

Optogenetic integration produces high-copy transgenes

We determined the copy number of the transgenes using quantitative PCR (qPCR). Extrachromosomal arrays are estimated to contain hundreds of copies of injected plasmids (Stinchcomb *et al.* 1985; Mello *et al.* 1991). We found that the copy number of optogenetically integrated transgenes was roughly correlated with the concentration of microinjected plasmids; the copy number of *Pttx-3-RFP* per haploid genome ranged from 129 to 576 when injected at 75 ng/μl, while those of *rol-6(su1006dm)* ranged from 31 to 144 when injected at 25 ng/μl (Figure 2A). In contrast to the variation of the copy number of each plasmid, the ratio between two plasmids from the same microinjection condition was consistent among independently isolated integrants (Figure 2B). This trend was also observed in another combination of plasmids (*Pttx-3-RFP* and *Prgef-1-GFP::efa-6N*, Figures 2C and 2D, see below). Thus, the optogenetic approach is suitable for integrating high-copy transgenic arrays and the desired copy number can be achieved by varying concentration of

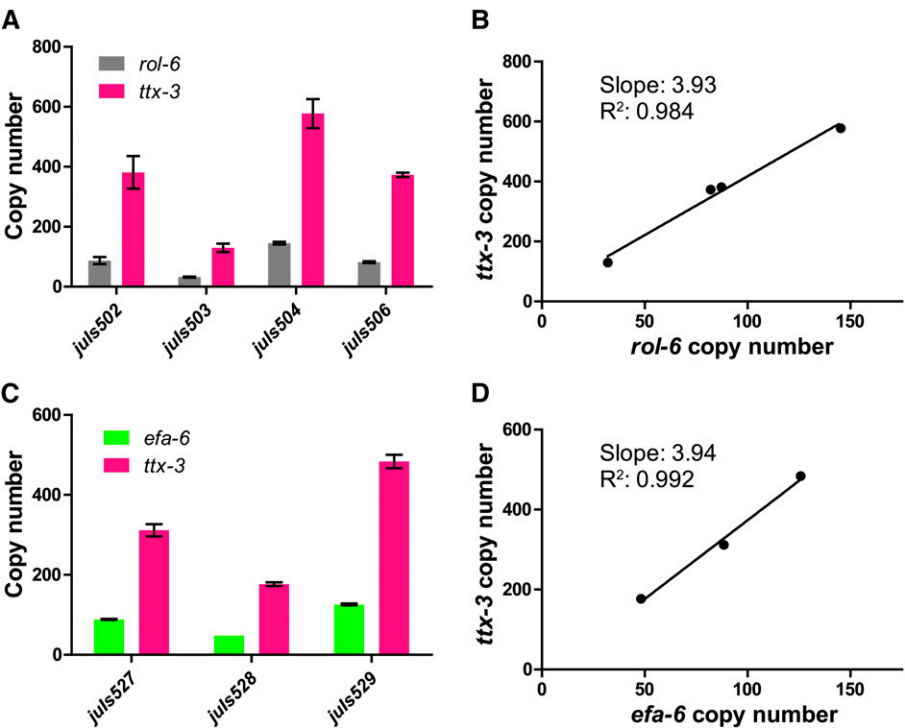


Figure 2 Copy number of optogenetically integrated transgenes. *rol-6(su1006dm)* at 25 ng/μl for (A) and (B) or *Prgef-1-GFP::efa-6N* at 25 ng/μl for (C) and (D) were microinjected with *Pttx-3-RFP* at 75 ng/μl. (A and C) The copy number was examined using quantitative PCR. Error bars indicate S.E.M. N = 2 biological replicates. (B and D) The ratio between two plasmids is consistent among different transgenes.

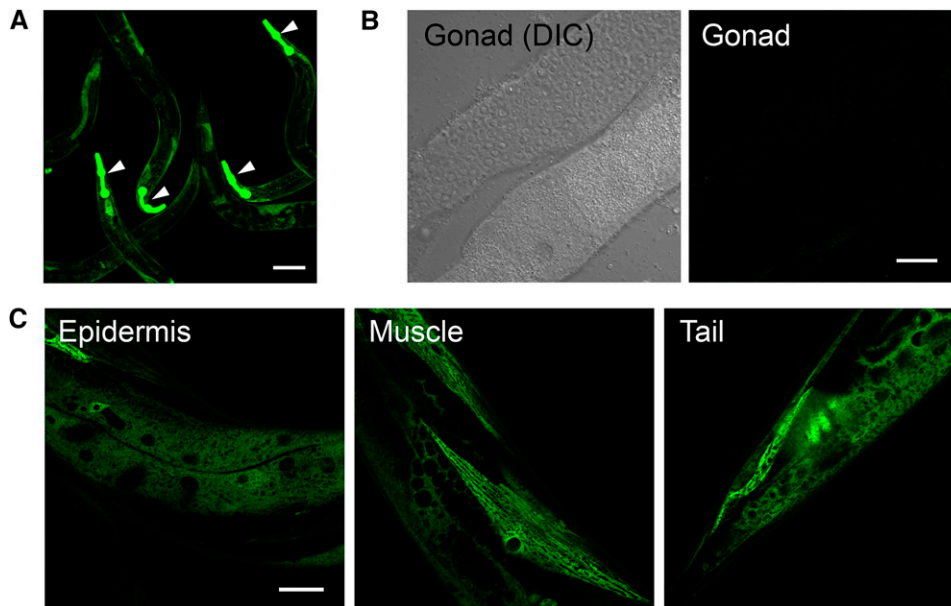


Figure 3 Optogenetically integrated transgenes are stably expressed. Expression of *juIs531*[GFP::*RPS-18*], which has one copy of integrated transgene in the background of *rps-18(ok3353)/nT1[qIs51 (Pmyo-2::GFP + Ppes-10::GFP + PF22B7.9::GFP)]*. (A) Live animals showing the stable expression among individuals. White arrowheads indicate the pharyngeal GFP signals expressed from nT1 balancer. (B) Dissected gonad showing the lack of expression. (C) Live animals showing the expression in the somatic tissues. Scale bars: 100 μ m in (A), 20 μ m in (B) and (C).

DNA plasmids. The high copy number and constant ratio of two co-injected plasmids suggest that a mixture of microinjected plasmids was integrated as a single transgenic array. Formation of extrachromosomal arrays appear to occur rapidly, within less than six hours, because we obtained integrants by light treatment six hours after microinjection.

Optogenetically integrated transgenes are stably expressed

We examined if optogenetically integrated transgenes showed consistency in expression level and pattern using a ubiquitously expressed ribosomal small subunit protein 18 (*rps-18*) (Noma *et al.* 2017). We generated two integrants expressing GFP-tagged *rps-18* with a co-injection marker *rol-6(su1006dm)* (*juIs531* and *juIs532* [*Prps-18-GFP::rps-18 + rol-6(su1006dm)*]). We detected consistent GFP::*RPS-18* expression among different individuals from a single parent (Figure 3A) in all somatic tissues (Figure 3C). We note, however, that other integrated transgenes, such as *juIs504* and *juIs505*[*rol-6(su1006dm) + Pttx-3-RFP*], showed stochastic expression of RFP in AIY, despite that *Rol* phenotype was 100% penetrant (Figure S1). This stochastic expression is probably not due to optogenetic integration protocol because variable expression is also reported in the integrants generated by traditional methods (Mello and Fire 1995). Since the insertion site in the genome is random in optogenetic integration, it is possible that integrated transgenes are silenced due to the position effect on the chromosome (Hsieh and Fire 2000). CRISPR-based insertion method might be used to incorporate multi-copy transgenes into a defined locus (Yoshina *et al.* 2016).

In *C. elegans* high-copy transgenes are often silenced in the germline cells (Kelly *et al.* 1997). We previously showed that a single copy GFP::*rps-18* transgene made by MosSCI technique is expressed in the germline (Noma *et al.* 2017). Here, we did not observe expression of GFP::*RPS-18* in the germline from two transgenes *juIs531* and *juIs532* that were generated by microinjecting *Prps-18-GFP::rps-18* plasmids at 1 ng/ μ l and had only one and six copies of GFP::*rps-18* per haploid genome, respectively. For reliable germline expression, optogenetic integration method

might be combined with complex arrays (Kelly *et al.* 1997) or introns with Periodic An/Tn-Clusters (PATCs) (Frøkjær-Jensen *et al.* 2016).

Optogenetic integration of transgenes toxic to organism development and/or function

Traditional methods for transgene integration require establishment of transgenic lines before mutagenesis, which is not suitable for integrating transgenes that cause sickness of worms. For example, overexpression of a dominant-interfering N-terminus of Exchange Factor for ARF-6 (EFA-6N) in neurons inhibits axon regeneration and perturbs neuronal development (Chen *et al.* 2011; Chen *et al.* 2015). While we could obtain extrachromosomal transgenes expressing the EFA-6N in all neurons, these worms had small brood size and displayed uncoordinated movement. In repeated efforts following UV/TMP method, we failed to obtain any integrants. We reasoned that optogenetic integration might overcome this problem because it bypasses the establishment of extrachromosomal transgenic lines. Indeed, from 24 injected P₀ using optogenetic integration, we successfully obtained four integrants of *Prgef-1-GFP::efa-6N*, which expresses GFP::EFA-6N under the control of pan-neuronal *rgef-1* promoter (Altun-Gultekin *et al.* 2001). Interestingly, different GFP::EFA-6N integrants had different degree of uncoordination (Figure 4A). We examined the relationship between the copy number and the fluorescence intensity or the uncoordinated behavior (Figure 4). The copy number was positively correlated with the fluorescence intensity (Figures 4B-D) and negatively with the speed of the worms (Figure 4E). Thus, the variation in copy number of optogenetic integration enables to address the dose-dependency of transgene expression. Similar to EFA-6N, overexpression of the active long isoform of dual-leucine zipper kinase (DLK-1L) in all neurons causes severe uncoordinated behavior (Nakata *et al.* 2005; Yan and Jin 2012), making it difficult to integrate extrachromosomal arrays with high expression level. Using optogenetic integration, we obtained one integrant expressing DLK-1L in all neurons (*knjIs1*[*Prgef-1-GFP::DLK-1L + Cbr-unc-119 + Pttx-3-RFP*]) from 12 P₀ animals, and these transgenic animals showed uncoordinated

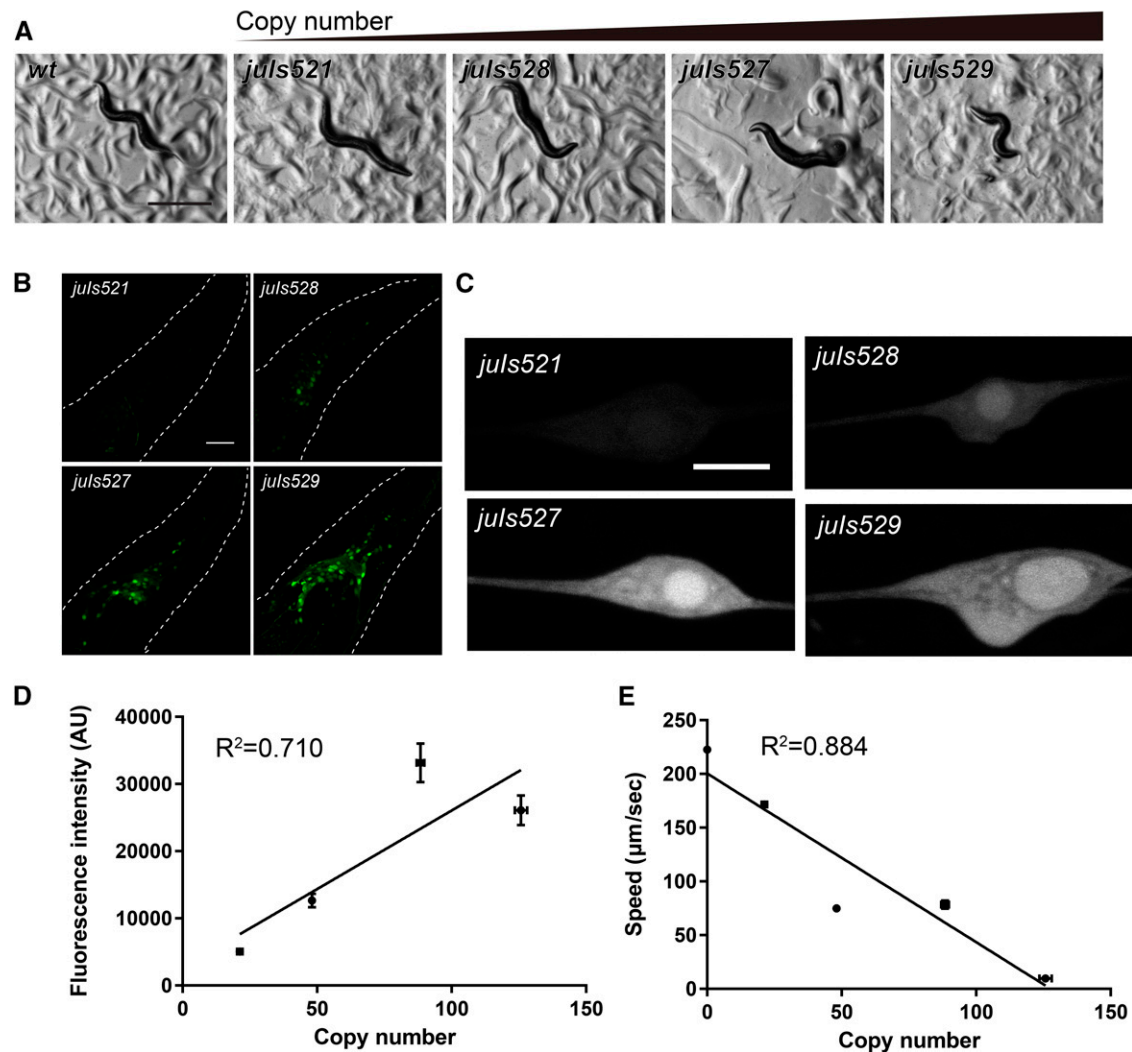


Figure 4 EFA-6N overexpression makes worm uncoordinated in a dose dependent manner. *Prgef-1*-GFP::EFA-6-N-terminus (GFP::EFA-6N) was overexpressed from the optogenetically integrated transgenes. (A) Bright field images of adult worms showing that overexpression of EFA-6N caused uncoordination depending on the copy number of integrated GFP::EFA-6N. Scale bar: 500 μ m. (B and C) Fluorescent images of the heads (B) and ALM neurons (C) showing different expression levels of GFP::EFA-6N. Dotted lines in (B) indicate the outlines of heads. Scale bars: 20 μ m in (B) and 5 μ m in (C). (D and E) Copy number of integrated transgenes was plotted against the fluorescence intensity in ALM neurons (D), and against the speed of worm locomotion (E). Error bars indicate S.E.M.

behavior (Figure S2 and Movie S1). Thus, optogenetic integration is suitable for the integration of transgenes with toxicity to organism development and/or function.

In summary, we have established a one-step optogenetic integration method that bypasses the need to first establish transgenic extrachromosomal arrays lines. This technical improvement has two benefits. One is significant reduction of time and labor for integration. Research using *C. elegans* has a strong demand on fast and efficient integration for rapid expansion of newly available reporters and genetic tools. For example, cGAL4-UAS system has recently become available in *C. elegans* community (Wang *et al.* 2017). To fully utilize this system, it is necessary to generate many different effector and promoter-driven GAL4 strains with high and stable expression. The second benefit is

that optogenetic integration makes it feasible to obtain integrants of high-copy transgenes that have toxic effects to organisms. Such transgenes are often desired in forward genetic screens to find the genetic modifiers of target genes (Wang and Sherwood 2011). For example, the generation of transgenes that fully mimic toxic effects of disease-causing mutations is useful for research using *C. elegans* as models for neurodegenerative diseases (Teschendorf and Link 2009; Markaki and Tavernarakis 2010).

ACKNOWLEDGMENTS

We would like to thank our laboratory members for testing the optogenetic integration methodology and for their comments on the

manuscript. This work was supported by PRESTO grant from Japan Science and Technology Agency to K.N. (JPMJPR168A), and by HHMI and NIH NS R37 035546 to Y.J.

LITERATURE CITED

- Altun-Gultekin, Z., Y. Andachi, E. L. Tsalik, D. Pilgrim, Y. Kohara *et al.*, 2001 A regulatory cascade of three homeobox genes, *ceh-10*, *ttx-3*, and *ceh-23*, controls cell fate specification of a defined interneuron class in *C. elegans*. *Development* 128: 1951–1969.
- Brenner, S., 1974 The genetics of *Caenorhabditis elegans*. *Genetics* 77: 71–94.
- Chen, L., M. Chuang, T. Koorman, M. Boxem, Y. Jin *et al.*, 2015 Axon injury triggers EFA-6 mediated destabilization of axonal microtubules via TACC and doublecortin like kinase. *eLife* 4. <https://doi.org/10.7554/eLife.08695>
- Chen, L., Z. Wang, A. Ghosh-Roy, T. Hubert, D. Yan *et al.*, 2011 Axon regeneration pathways identified by systematic genetic screening in *C. elegans*. *Neuron* 71: 1043–1057. <https://doi.org/10.1016/j.neuron.2011.07.009>
- Evans, T. C., 2006 Transformation and microinjection. *WormBook* ed. The *C. elegans* Research Community, *WormBook*. <https://doi.org/10.1895/wormbook.1.108.1>
- Frøkjær-Jensen, C., M. W. Davis, C. E. Hopkins, B. J. Newman, J. M. Thummel *et al.*, 2008 Single-copy insertion of transgenes in *Caenorhabditis elegans*. *Nat. Genet.* 40: 1375–1383. <https://doi.org/10.1038/ng.248>
- Frøkjær-Jensen, C., M. W. Davis, M. Sarov, J. Taylor, S. Flibotte *et al.*, 2014 Random and targeted transgene insertion in *Caenorhabditis elegans* using a modified Mos1 transposon. *Nat. Methods* 11: 529–534. <https://doi.org/10.1038/nmeth.2889>
- Frøkjær-Jensen, C., N. Jain, L. Hansen, M. W. Davis, Y. Li *et al.*, 2016 An Abundant Class of Non-coding DNA Can Prevent Stochastic Gene Silencing in the *C. elegans* Germline. *Cell* 166: 343–357. <https://doi.org/10.1016/j.cell.2016.05.072>
- Holland, S. M., K. M. Collura, A. Ketschek, K. Noma, T. A. Ferguson *et al.*, 2016 Palmitoylation controls DLK localization, interactions and activity to ensure effective axonal injury signaling. *Proc. Natl. Acad. Sci. USA* 113: 763–768. <https://doi.org/10.1073/pnas.1514123113>
- Hsieh, J., and A. Fire, 2000 Recognition and silencing of repeated DNA. *Annu. Rev. Genet.* 34: 187–204. <https://doi.org/10.1146/annurev.genet.34.1.187>
- Kelly, W. G., S. Xu, M. K. Montgomery, and A. Fire, 1997 Distinct requirements for somatic and germline expression of a generally expressed *Caenorhabditis elegans* gene. *Genetics* 146: 227–238.
- Kim, H., T. Ishidate, K. S. Ghanta, M. Seth, D. Conte, Jr *et al.*, 2014 A co-CRISPR strategy for efficient genome editing in *Caenorhabditis elegans*. *Genetics* 197: 1069–1080. <https://doi.org/10.1534/genetics.114.166389>
- Markaki, M., and N. Tavernarakis, 2010 Modeling human diseases in *Caenorhabditis elegans*. *Biotechnol. J.* 5: 1261–1276. <https://doi.org/10.1002/biot.201000183>
- Mello, C., and A. Fire, 1995 DNA transformation. *Methods Cell Biol.* 48: 451–482. [https://doi.org/10.1016/S0091-679X\(08\)61399-0](https://doi.org/10.1016/S0091-679X(08)61399-0)
- Mello, C. C., J. M. Kramer, D. Stinchcomb, and V. Ambros, 1991 Efficient gene transfer in *C. elegans*: extrachromosomal maintenance and integration of transforming sequences. *EMBO J.* 10: 3959–3970.
- Nakata, K., B. Abrams, B. Grill, A. Goncharov, X. Huang *et al.*, 2005 Regulation of a DLK-1 and p38 MAP kinase pathway by the ubiquitin ligase RPM-1 is required for presynaptic development. *Cell* 120: 407–420. <https://doi.org/10.1016/j.cell.2004.12.017>
- Noma, K., A. Goncharov, M. H. Ellisman, and Y. Jin, 2017 Microtubule-dependent ribosome localization in *C. elegans* neurons. *eLife* 6: e26376. <https://doi.org/10.7554/eLife.26376>
- Noma, K., and Y. Jin, 2015 Optogenetic mutagenesis in *Caenorhabditis elegans*. *Nat. Commun.* 6: 8868. <https://doi.org/10.1038/ncomms9868>
- Noma, K., and Y. Jin, 2016 Optogenetic Random Mutagenesis Using Histone-miniSOG in *C. elegans*. *J. Vis. Exp.* 117: e54810, 1–7. <https://doi.org/10.3791/54810>
- Paix, A., A. Folkmann, D. Rasoloson, and G. Seydoux, 2015 High Efficiency, Homology-Directed Genome Editing in *Caenorhabditis elegans* Using CRISPR-Cas9 Ribonucleoprotein Complexes. *Genetics* 201: 47–54. <https://doi.org/10.1534/genetics.115.179382>
- Paix, A., Y. Wang, H. E. Smith, C. Y. Lee, D. Calidas *et al.*, 2014 Scalable and versatile genome editing using linear DNAs with microhomology to Cas9 Sites in *Caenorhabditis elegans*. *Genetics* 198: 1347–1356. <https://doi.org/10.1534/genetics.114.170423>
- Schindelin, J., I. Arganda-Carreras, E. Frise, V. Kaynig, M. Longair *et al.*, 2012 Fiji: an open-source platform for biological-image analysis. *Nat. Methods* 9: 676–682. <https://doi.org/10.1038/nmeth.2019>
- Shu, X., V. Lev-Ram, T. J. Deerinck, Y. Qi, E. B. Ramko *et al.*, 2011 A genetically encoded tag for correlated light and electron microscopy of intact cells, tissues, and organisms. *PLoS Biol.* 9: e1001041. <https://doi.org/10.1371/journal.pbio.1001041>
- Stinchcomb, D. T., J. E. Shaw, S. H. Carr, and D. Hirsh, 1985 Extrachromosomal DNA transformation of *Caenorhabditis elegans*. *Mol. Cell. Biol.* 5: 3484–3496. <https://doi.org/10.1128/MCB.5.12.3484>
- Teschendorf, D., and C. D. Link, 2009 What have worm models told us about the mechanisms of neuronal dysfunction in human neurodegenerative diseases? *Mol. Neurodegener.* 4: 38. <https://doi.org/10.1186/1750-1326-4-38>
- Wang, H., J. Liu, S. Gharib, C. M. Chai, E. M. Schwarz *et al.*, 2017 cGAL, a temperature-robust GAL4-UAS system for *Caenorhabditis elegans*. *Nat. Methods* 14: 145–148. <https://doi.org/10.1038/nmeth.4109>
- Wang, Z., and D. R. Sherwood, 2011 Dissection of genetic pathways in *C. elegans*. *Methods Cell Biol.* 106: 113–157. <https://doi.org/10.1016/B978-0-12-544172-8.00005-0>
- Yan, D., and Y. Jin, 2012 Regulation of DLK-1 Kinase Activity by Calcium-Mediated Dissociation from an Inhibitory Isoform. *Neuron* 76: 534–548. <https://doi.org/10.1016/j.neuron.2012.08.043>
- Yoshina, S., Y. Suhehiro, E. Kage-Nakadai, and S. Mitani, 2016 Locus-specific integration of extrachromosomal transgenes in *C. elegans* with the CRISPR/Cas9 system. *Biochem. Biophys. Rep.* 5: 70–76. <https://doi.org/10.1016/j.bbrep.2015.11.017>

Communicating editor: B. Andrews